The Astrophysical Journal, 614:386–397, 2004 October 10

SPECTROSCOPY OF VERY LOW MASS STARS AND BROWN DWARFS IN IC 2391: LITHIUM DEPLETION AND Hα EMISSION

David Barrado y Navascués
Laboratorio de Astrofísica Espacial y Física Fundamental, INTA, P.O. Box 50727, E-2808 Madrid, Spain; barrado@laeff.esa.es

John R. Stauffer
IPAC, California Institute of Technology, Pasadena, CA 91125; stauffer@ipac.caltech.edu

and

Ray Jayawardhana
Department of Astronomy and Astrophysics, University of Toronto, 60 St. George Street, Toronto, Ontario M5S 3H8, Canada; rayjay@astro.utoronto.ca
Received 2004 January 21; accepted 2004 June 21

ABSTRACT

We have obtained intermediate-resolution optical spectroscopy of 44 candidate very low mass members of the nearby young open cluster IC 2391. Of these, 26 spectra are totally new, 14 had been analyzed in a previous paper, and another four are in common with that paper. These spectra, taken at the Cerro Tololo 4 m and Magellan I and II telescopes, allow us to confirm 33 of them as likely cluster members, based on their spectral types, the presence of Li, and Hα emission. Among these new cluster members is CTIO-160 (M7), the first IC 2391 candidate to satisfy all criteria for being a substellar member of the cluster, including detection of the Li 6708 Å doublet. With the enlarged membership, we are able to locate the lithium depletion boundary of the cluster more reliably than in the past. On the basis of comparison of several theoretical models, we derive an age of 50 ± 5 Myr for IC 2391. We also estimate new ages for the α Per and Pleiades clusters; our ages are 85 ± 10 and 130 ± 20 Myr, respectively. We derive an estimate of the initial mass function of IC 2391 that extends to below the substellar limit and compare it to those of other well-studied young open clusters. The index of the power-law mass function for IC 2391 is $\alpha = 0.96 \pm 0.12$, valid in the range 0.5–0.072 $M_\odot$.

Subject headings: open clusters and associations: individual (IC 2391) — stars: low-mass, brown dwarfs — stars: luminosity function, mass function — stars: pre–main-sequence

1. INTRODUCTION

Hundreds of open clusters[1] are known in the Galaxy. However, few among them are well characterized (size, distance, and reddening), and fewer still are close enough to allow their stellar population to be investigated in detail. Only the Pleiades, the Hyades, α Per, and a few other clusters have been systematically studied. Our goal is to add other clusters to this list, and IC 2391 has been the focus of some of our efforts.

IC 2391 is a young cluster with an estimated age, based on main-sequence isochrone fitting, of 35 Myr (Mermilliod 1981). It is one of the nearest clusters, with a *Hipparcos* distance modulus of $(m-M)_0 = 5.82 \pm 0.07$ (Robichon et al. 1999). The interstellar reddening in its direction is very low, $E(B-V) = 0.04$ or 0.06, as estimated by Becker & Fenkart (1971) and Patten & Simon (1996), respectively. This last work also estimated a distance of $(m-M)_0 = 5.95 \pm 0.10$, which is the value we use here.

In Barrado y Navascués et al. (1999, hereafter Paper I), we presented some spectra of very low mass members of the cluster and a preliminary age estimate, 53 Myr, based on the lithium depletion technique (see Stauffer et al. 1998; Basri et al. 1996). Subsequently, in Barrado y Navascués et al. (2001c, hereafter Paper II), we conducted an extensive photometric survey in the optical that yielded a substantial population of candidate members, both very low mass stars and brown dwarfs. The combination of this database with infrared photometry from Two Micron All Sky Survey (2MASS; Skrutskie et al. 1997; see also Cutri et al. 2003) allowed us to extract from the initial sample those objects that might be interlopers, based on the analysis of different color-magnitude and color-color diagrams. In the introduction to Paper II, we described the results achieved by previous studies, namely, those papers that looked for new cluster members more massive than those presented in Paper II, and those papers that studied the properties of true cluster members (X-ray emission, rotation, lithium abundance, and so on). Since then, the only other works that have been published dealing with properties of members of this cluster are Randich et al. (2001) on spectra and Allen et al. (2003) on the luminosity function (LF) and the age.

Here we present medium-resolution optical spectra of a large number of candidate members discovered in Paper II and consider the membership of those candidates by studying their spectral types, Hα emission, and sodium and lithium content; we derive again, in a more accurate way thanks to the larger number of objects, the location of the lithium depletion boundary (LDB) of the cluster and hence its age; and we study the initial mass function (IMF).

2. OBSERVATIONS

2.1. *Sample*

The spectra presented in this paper correspond to IC 2391 candidate members discovered by two different groups. The first (generally brighter) set was selected from Patten & Simon

[1] A comprehensive database has been collected by J.-C. Mermilliod and can be found at http://obswww.unige.ch/webda.

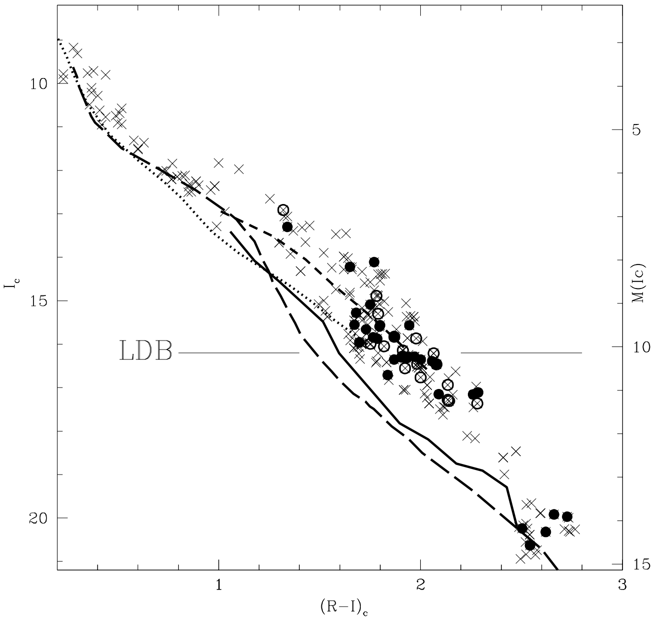

FIG. 1.—CMD for IC 2391 candidate members. Crosses represent all the available photometric data from Patten & Simon (1996), Patten & Pavlovsky (1999), and Barrado y Navascués et al. (2001c). Open circles correspond to spectroscopic data from Barrado y Navascués et al. (1999), whereas filled circles were observed with Hydra II or the Magellan I and II Telescopes. We plot different 50 Myr isochrones (short-dashed line for D'Antona & Mazzitelli 1997, long-dashed line for Baraffe et al. 1998, and dotted line for Siess et al. 2000). The solid line represents an empirical ZAMS.

(1996) and Patten & Pavlovsky (1999). The second group was extracted from Paper II, in which we presented a large sample of low-mass stars and brown dwarf candidates in the range $12 < I_C < 21$, discovered in a deep optical and infrared photometric search. An initial subset of this survey was previously published in Paper I, and it includes medium-resolution spectroscopy, allowing the confirmation of the membership of most of them. These spectra were obtained in 1999 January with the Ritchey-Chrétien spectrograph at the Cerro Tololo Interamerican Observatory (CTIO) 4 m telescope and have a spectral resolution equivalent to 2.7 Å (see Paper I for details).

In the present study, we have carried out spectroscopic observations at medium resolution for a total of 44 candidate members. Of these, 26 have been observed for the first time, while 18 were already analyzed in Paper I. Four of these 18 have been reobserved. We especially selected those objects located around the LDB in a color-magnitude diagram (CMD; generally very cool stars with masses slightly larger than the substellar limit at 0.072 $M_\odot$). Figure 1 displays the I magnitude versus the $(R - I)$ color in the Cousins system. Proposed IC 2391 members are included as crosses. Open circles represent those candidates with spectra (in some cases at quite low signal-to-noise ratio [S/N]) from Paper I, whereas candidates with new spectroscopic data are illustrated with filled circles in the diagram. An empirical zero-age main sequence (ZAMS) from Barrado y Navascués et al. (2001b) is displayed as a solid line, as well as several 50 Myr isochrones (Baraffe et al. 1998; Siess et al. 2000; D'Antona & Mazzitelli 1997; *long-dashed, dotted, and short-dashed lines, respectively*). The location of the LDB estimated in Paper I is also included. Because of the lack of space and since the main goal of Paper I was to establish the location of the LDB of the cluster, we did not publish all the spectra of that sample. We now present them in Figure 2.

Table 1 lists all the targets observed in both Paper I (except the three nonmembers analyzed there) and in this paper and includes accurate position (from the 2MASS survey; Cutri et al. 2003), optical as well as near-infrared photometry, and information regarding how the spectra were collected (telescope, instrument, and date).

2.2. *Multifiber Spectroscopy from CTIO*

On 1999 March 10 and 13, we collected multifiber medium-resolution spectroscopy with the Hydra II bench spectrograph at the CTIO 4 m telescope under a shared risk program. The

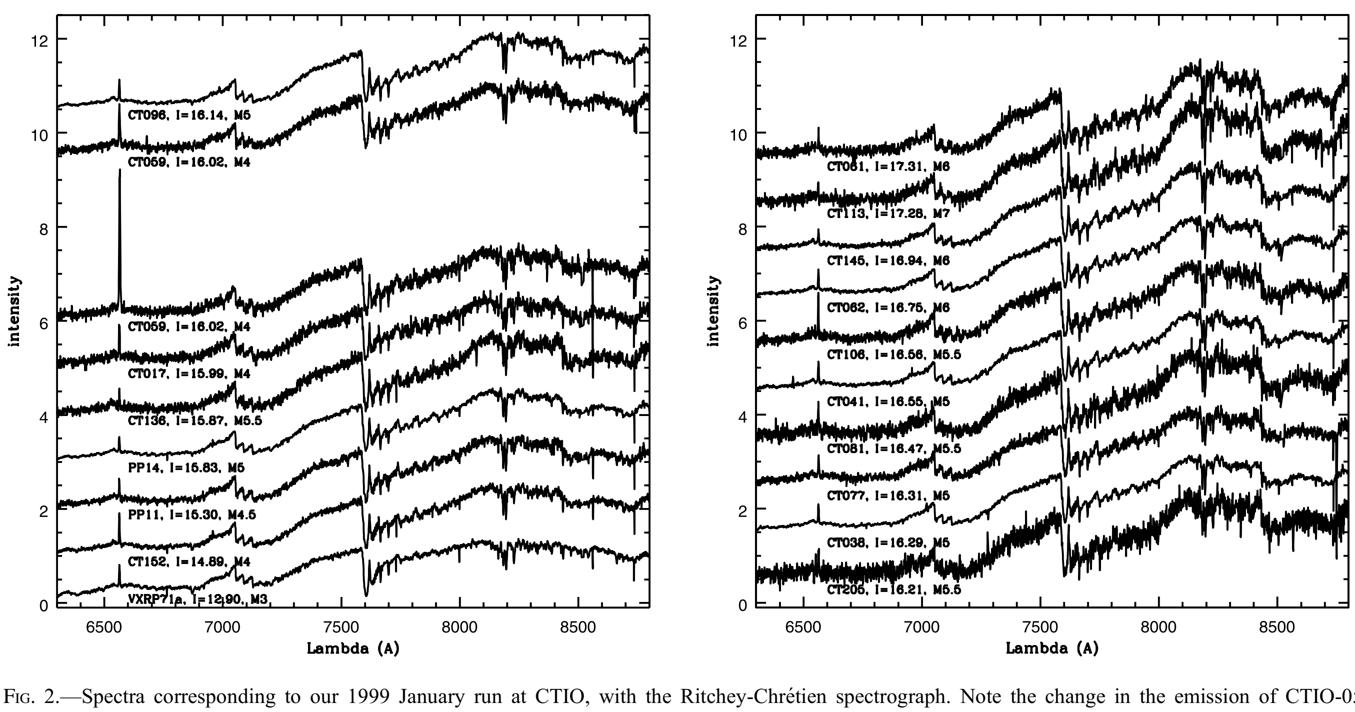

FIG. 2.—Spectra corresponding to our 1999 January run at CTIO, with the Ritchey-Chrétien spectrograph. Note the change in the emission of CTIO-059, probably due to a flare.

TABLE 1
Photometry for our IC 2391 Targets

Name	R.A. (2000.0)	Decl. (2000.0)	V	I_c	$(R-I)_C$	J	H	K_s	Run[a]
VXRP39a	8 41 51.54	−53 20 59.7	15.74	13.30	1.34	12.049	11.392	11.179	CTIO/HYDRA II
VXRP71a	8 44 19.08	−53 08 28.9	15.32	12.91	1.32	11.672	11.069	10.795	CTIO/R&C
PP 02	8 39 05.67	−53 21 44.6	17.15	14.22	1.65	12.723	12.098	11.848	CTIO/HYDRA II
PP 07	8 39 29.58	−53 21 04.4	17.31	14.11	1.77	12.480	11.883	11.615	CTIO/HYDRA II
PP 11	8 44 04.65	−53 00 01.7	18.48	15.30	1.79	13.684	13.075	12.810	CTIO/R&C
PP 14	8 40 30.31	−53 11 30.9	19.22	15.83	1.87	14.184	13.589	13.294	CTIO/R&C,CTIO/HYDRA II
CTIO-002	8 35 44.88	−53 25 55.7	...	17.157	2.260	16.367	14.234	14.035	Magellan/B&C
CTIO-012	8 36 45.72	−53 11 32.6	18.78	15.553	1.672	13.935	13.251	12.992	Magellan/B&C
CTIO-017	8 37 11.46	−52 36 35.7	19.30	15.989	1.752	14.461	13.860	13.587	CTIO/R&C
CTIO-026	8 37 18.19	−52 55 56.9	...	16.352	2.001	14.507	13.880	13.492	Magellan/MIKE
CTIO-038	8 37 59.20	−53 21 55.4	19.90	16.291	1.910	14.455	13.869	13.643	CTIO/R&C,CTIO/HYDRA II
CTIO-041	8 38 11.89	−52 22 51.4	20.46	16.554	1.923	14.630	14.088	13.741	CTIO/R&C
CTIO-046	8 38 25.10	−53 19 10.9	18.92	15.958	1.697	14.420	13.803	13.435	CTIO/HYDRA II
CTIO-049	8 38 27.15	−53 25 10.4	19.05	15.566	1.944	13.928	13.336	13.002	CTIO/HYDRA II
CTIO-054	8 38 36.10	−53 25 52.1	...	20.629	2.542	...	...	...	CTIO/HYDRA II
CTIO-056	8 38 38.80	−53 07 57.5	...	16.711	1.837	15.314	14.631	14.365	CTIO/HYDRA II
CTIO-058	8 38 42.34	−53 29 31.3	...	19.919	2.661	...	...	...	CTIO/HYDRA II
CTIO-059	8 38 44.03	−53 22 51.0	19.47	16.050	1.819	14.460	13.757	13.526	CTIO/R&C
CTIO-061	8 38 47.07	−52 14 56.4	...	17.309	2.141	15.274	14.677	14.206	CTIO/R&C
CTIO-062	8 38 47.30	−52 44 32.7	20.84	16.765	2.000	14.954	14.389	13.989	CTIO/R&C
CTIO-067	8 38 56.19	−52 51 38.1	...	17.111	2.285	16.087	15.626	15.795	Magellan/B&C
CTIO-073	8 39 32.06	−53 28 12.7	...	20.322	2.620	...	...	...	CTIO/HYDRA II
CTIO-074	8 39 40.59	−53 06 07.7	...	15.876	1.786	14.191	13.526	13.278	CTIO/HYDRA II
CTIO-076	8 39 48.45	−53 13 58.5	18.47	15.278	1.681	13.664	13.045	12.745	CTIO/HYDRA II
CTIO-077	8 40 09.53	−53 37 49.7	20.04	16.308	1.929	14.543	13.962	13.632	CTIO/R&C,CTIO/HYDRA II
CTIO-081	8 40 14.77	−53 27 36.4	20.38	16.465	2.079	14.370	13.745	13.394	CTIO/R&C,CTIO/HYDRA II
CTIO-083	8 40 16.07	−53 25 47.9	18.85	15.565	1.799	13.906	13.272	12.933	CTIO/HYDRA II
CTIO-087	8 40 42.92	−53 09 19.0	...	20.240	2.503	...	...	...	CTIO/HYDRA II
CTIO-089	8 40 46.81	−53 13 52.1	...	19.971	2.726	...	...	...	CTIO/HYDRA II
CTIO-091	8 40 53.00	−52 23 00.4	...	15.842	1.765	14.082	13.460	13.174	Magellan/B&C
CTIO-096	8 41 12.38	−53 09 10.3	19.75	16.144	1.912	14.344	13.818	13.404	CTIO/R&C
CTIO-097	8 41 26.00	−53 26 34.8	...	15.087	1.751	13.456	12.761	12.541	CTIO/HYDRA II
CTIO-098	8 41 29.18	−53 16 22.3	18.87	15.593	1.797	13.988	13.333	13.060	CTIO/HYDRA II
CTIO-106	8 41 58.93	−53 12 36.4	...	16.454	1.983	14.655	13.997	13.676	CTIO/R&C
CTIO-113	8 42 18.71	−52 39 40.1	21.9	17.282	2.135	15.083	14.377	14.030	CTIO/R&C
CTIO-136	8 43 15.15	−52 58 23.0	19.72	15.868	1.978	14.134	13.482	13.129	CTIO/R&C
CTIO-145	8 43 23.67	−53 14 16.9	...	16.936	2.135	15.059	14.386	13.962	CTIO/R&C
CTIO-152	8 43 38.42	−52 50 55.6	18.11	14.891	1.781	13.337	12.714	12.452	CTIO/R&C
CTIO-160	8 44 02.10	−52 44 10.7	21.05	17.151	2.090	15.115	14.468	14.103	Magellan/B&C
CTIO-192	8 45 02.58	−52 59 28.8	...	16.286	1.970	14.460	13.853	13.527	Magellan/MIKE
CTIO-195	8 45 45.60	−53 12 37.8	...	16.353	1.869	14.566	13.986	13.611	Magellan/MIKE
CTIO-202	8 46 26.27	−53 01 53.5	...	16.391	2.057	14.472	13.962	13.551	Magellan/MIKE
CTIO-205	8 47 03.47	−52 46 52.3	20.21	16.211	2.065	14.217	13.744	13.350	CTIO/R&C
CTIO-206	8 40 40.84	−53 13 31.9	...	15.658	1.730	13.697	13.132	12.785	CTIO/HYDRA II

Note.—Units of right ascension are hours, minutes, and seconds, and units of declination are degrees, arcminutes, and arcseconds.
[a] CTIO/R&C: 1999 January (Paper I); CTIO/HYDRA II: 1999 March 10–13; Magellan/B&C: 2003 March 11; Magellan/MIKE: 2002 December 11–14.

grating KPGL-D was used with the OG-570 filter. The achieved resolution was 2.7 Å as measured in ThAr comparison spectra observed with the same set-up and covering the spectral range 6300–8500 Å.

The total exposure time was 11.5 hr, but we divided this time into 12 individual observations of 1 hr each (except the last one, which lasted only 30 minutes) during these two nights. Each exposure was processed individually with the IRAF[2] package "HYDRA." We used dome flats. After the extraction of each one-dimensional spectrum and its calibration in wavelength, we combined all the data corresponding to the same target into a final spectrum using a median algorithm in order to remove the hits by cosmic rays. No correction for telluric lines or instrumental profile was carried out. The final spectra can be seen in Figure 3.

2.3. *Spectroscopy from Magellan I and II*

During two different observing runs mainly devoted to other goals, we were able to complement the previous data with additional spectra collected at the Magellan 6.5 m twin telescopes, located at Las Campanas Observatory. The first campaign took place 2002 December 11–14th. We used Magellan I and the MIKE echelle spectrograph. MIKE provides spectral resolution that is actually too high for our purposes. For this

[2] IRAF is distributed by National Optical Astronomy Observatories, which is operated by the Association of Universities for Research in Astronomy, Inc., under contract to the National Science Foundation.

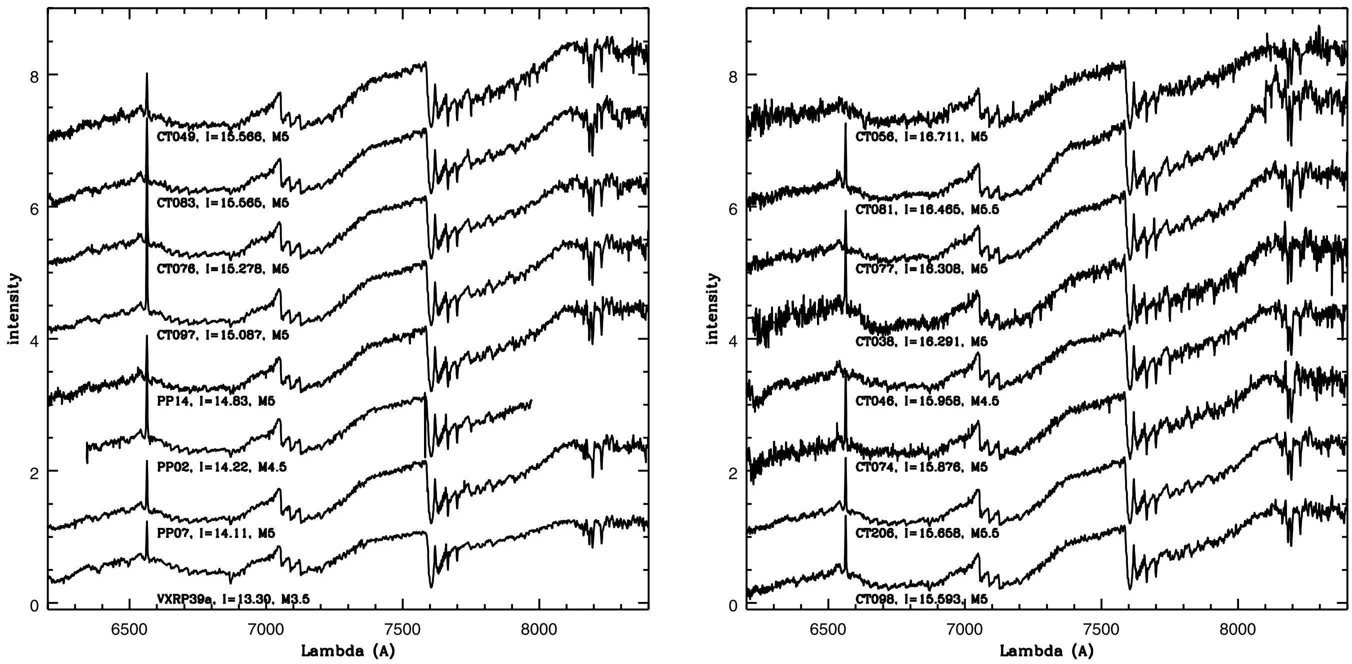

FIG. 3.—Spectra collected with CTIO+Hydra II during our 1999 March run.

reason and in order to improve the final S/N, we degraded the resolution by rebinning the original data during the readout to 2 and 8 pixels in the spatial and spectral directions, respectively, thus obtaining spectra with a resolution of 0.55 Å and complete spectral coverage of 4500–7250 Å. Four IC 2391 candidate member were observed with MIKE. We show the Hα order from these spectra in Figure 4*a*. The second run took place on 2003 March 11; five additional candidates were observed, in this case with Magellan II and the B&C spectrograph, using the 1200 line mm^{-1} grating, yielding a 2.3 Å resolution. These last spectra can be seen in Figure 4*b* (probable nonmembers are not included in the diagram). In most cases, we took three individual exposures of 1200 s each, fully reduced each exposure separately, and then added together the three resultant one-dimensional spectra at the end. Additional details can be found in Barrado y Navascués et al. (2004).

3. ANALYSIS

Table 2 lists our results, including the derived spectral type, the measured Hα, sodium and lithium equivalent widths at 6563, 8200, and 6708 Å, respectively, and the estimated effective temperature and lithium abundance. We used calibrations by Bessell (1979), Leggett (1992), and Basri et al. (2000), the $(R-I)_C$ color and spectral types for the $T_{\rm eff}$ determination,

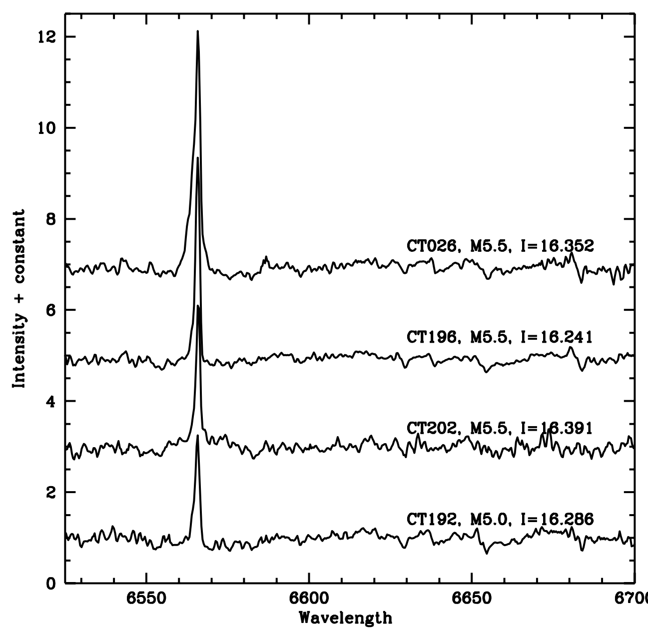

FIG. 4*a*

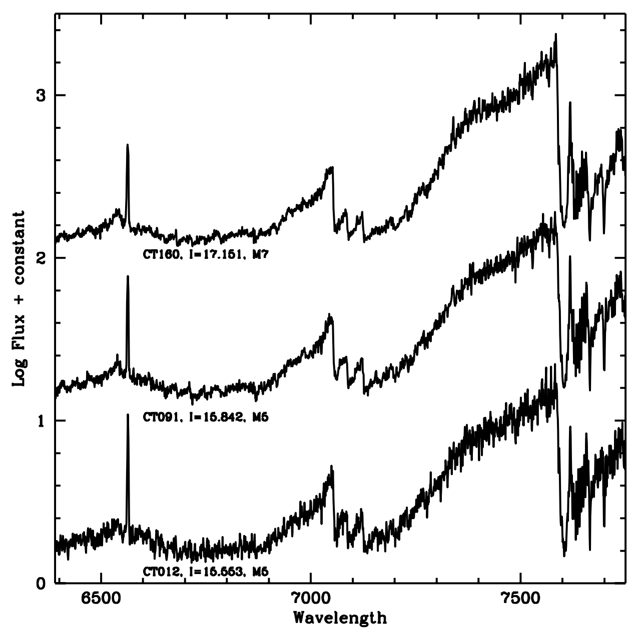

FIG. 4*b*

FIG. 4.—(*a*) 2002 December spectra taken with the Magellan I Telescope and the MIKE echelle spectrograph. We only show the order corresponding to the Hα line. Note that the continuum has been normalized. (*b*) 2003 March spectra (only members) taken with the Magellan II Telescope and the B&C spectrograph.

TABLE 2

Spectroscopy Data for IC 2391 Candidate Members

Name	I_c	$W(\mathrm{H}\alpha)$[a] (Å)	$W(\mathrm{Na})$[b] (Å)	$W(\mathrm{Li})$[b] (Å)	$A(\mathrm{Li})$	T_{eff}[c] (K)	T_{eff}[d] (K)	Spectral Type	Member?
VXRP39a	13.30	3.8 ± 0.3	4.3 ± 0.1	<0.03	<0.00	3515	3250	M3.5	Yes
VXRP71a	12.91	4.9 ± 0.3	...	<0.10	<0.00	3560	3350	M3.0	Yes
PP 02	14.22	8.9 ± 0.6	3.5 ± 0.6	<0.04	<0.00	3149	3075	M4.5	Yes
PP 07	14.11	7.1 ± 0.7	5.0 ± 0.2	0.23 ± 0.09	0.89	3063	3000	M5.0	Yes?
PP 11	15.30	5.4 ± 0.5	4.7 ± 0.2	<0.06	<0.00	3044	3075	M4.5	Yes
PP 14	15.83	1.4/6.3 ± 0.2/0.3	5.4 ± 0.2	<0.03	<0.00	2983	3000	M5.0	Yes
CTIO-002	17.157	−3.0	Out[e]	...	...	2645	...	K	NM
CTIO-012	15.553	13.4 ± 0.7	Out[e]	<0.20	<0.00	3122	3000	M5.0	Yes
CTIO-017	15.989	11.0 ± 1.1	5.6 ± 0.2	<0.12	<0.00	3081	3150	M4.0	Yes
CTIO-026	16.352	19.9 ± 2.5	Out[e]	0.37 ± 0.08	1.17	2858	2900	M5.5	Yes
CTIO-038	16.291	0.6/7.0 ± 1.0/0.5	5.0 ± 0.5	0.53 ± 0.09	2.53	2966	3000	M5.0	Yes
CTIO-041	16.554	8.7 ± 0.8	5.2 ± 0.2	0.53 ± 0.15	2.53	2962	3000	M5.0	Yes
CTIO-046	15.958	<0	7.3 ± 0.2	<0.07	<0.00	3127	3075	M4.5	NM
CTIO-049	15.566	0.4 ± 0.2	5.8 ± 0.6	<0.02	<0.00	2956	3000	M5.0	Yes
CTIO-054	20.629	<0	...	...	...	...	...	...	NM
CTIO-056	16.711	17.0 ± 2.2	5.6 ± 0.6	...	...	3003	3000	M5.0	Yes
CTIO-058	19.919	<0	...	...	...	...	...	...	NM
CTIO-059	16.050	34.1±1.6[f]	5.6 ± 0.2	<0.15	<0.00	3017	3150	M4.0	Yes
CTIO-061	17.309	2.3 ± 1.0	5.9 ± 0.3	...	...	2801	2800	M6.0	Yes
CTIO-062	16.765	7.2 ± 1.0	5.3 ± 0.3	0.42 ± 0.15	1.64	2937	2800	M6.0	Yes
CTIO-067	17.111	−2.5	Out[e]	...	...	2603	...	K	NM
CTIO-073	20.322	<0	...	...	...	...	...	...	NM
CTIO-074	15.876	5.9 ± 0.6	6.4 ± 1.0	<0.04	<0.00	3048	3000	M5.0	Yes
CTIO-076	15.278	11.2 ± 0.7	4.9 ± 0.3	<0.02	<0.00	3137	3000	M5.0	Yes
CTIO-077	16.308	7.0/7.4 ± 0.9/0.3	5.5 ± 0.3	1.2 ± 0.4[g]	3.4	2960	3000	M5.0	Yes
CTIO-081	16.465	0.7/8.6 ± 0.1/0.3	6.0 ± 0.4	0.82 ± 0.15	3.4	2885	2900	M5.5	Yes[h]
CTIO-083	15.565	10.9 ± 0.3	5.5 ± 0.4	<0.01	<0.00	3035	3000	M5.0	Yes
CTIO-087	20.240	Emission[i]	...	...	...	...	...	...	Yes?
CTIO-089	19.971	Emission[i]	...	...	...	...	...	...	Yes?
CTIO-091	15.842	9.9 ± 0.8	5.7 ± 0.4	<0.10	<0.00	3035	3000	M5.0	Yes
CTIO-096	16.144	8.7 ± 0.7	5.3 ± 0.2	<0.10	<0.00	2966	3000	M5.0	Yes
CTIO-097	15.087	7.3 ± 1.3	5.7 ± 0.3	<0.01	<0.00	3082	3000	M5.0	Yes
CTIO-098	15.593	2.0 ± 0.2	5.5 ± 0.4	<0.01	<0.00	3037	3000	M5.0	Yes
CTIO-106	16.454	14.1 ± 1.8	5.8 ± 0.3	...	...	2944	2900	M5.5	Possible
CTIO-113	17.282	4.6 ± 1.0	6.3 ± 0.5	...	...	2812	2575	M7.0	Yes
CTIO-136	15.868	6.1 ± 0.9	5.2 ± 0.2	<0.10	<0.00	2945	2900	M5.5	Yes
CTIO-145	16.936	7.9 ± 2.9	5.5 ± 0.3	0.48 ± 0.11	1.96	2812	2800	M6.0	Yes
CTIO-152	14.891	9.9 ± 0.6	5.1 ± 0.3	<0.02	<0.00	3053	3150	M4.0	Yes
CTIO-160	17.151	12.0 ± 1.8	Out[e]	0.9 ± 0.2	3.4	2806	2575	M7.0	Yes
CTIO-192	16.286	5.3 ± 0.4	Out[e]	0.40 ± 0.15	1.40	2876	3000	M5.0	Yes
CTIO-195	16.353	9.8 ± 1.5	Out[e]	0.56 ± 0.12	2.75	2941	2900	M5.5	Yes
CTIO-202	16.391	6.1 ± 1.5	Out[e]	...	...	2826	2900	M5.5	Yes
CTIO-205	16.211	8.0 ± 6.2	5.2 ± 0.6	...	...	2898	2900	M5.5	Yes?
CTIO-206	15.658	7.4 ± 0.8	5.9 ± 0.4	0.42 ± 0.11	0.95	3101	2900	M5.5	Yes

[a] $W(\mathrm{H}\alpha) > 0$ correspond to emission, whereas negative values correspond to absorption.
[b] All $W(\mathrm{Na\ I}\ \lambda8200)$ and $W(\mathrm{Li\ I}\ \lambda6708)$ are in absorption.
[c] T_{eff} from $(R-I)_{\mathrm{C}}$ color.
[d] T_{eff} from the spectral type.
[e] Na I $\lambda8200$ out of range.
[f] Average of two observations on consecutive nights. The individual values are $W(\mathrm{H}\alpha) = 45.5$ and 18.8 Å.
[g] The detection of lithium is quite uncertain in this case.
[h] Classified as "possible" member in Paper I. We have collected a higher S/N spectrum, which indicates the presence of lithium.
[i] In emission, with no continuum (very low S/N).

and curves of growth by Zapatero Osorio et al. (2002) for the lithium abundance. In the subsequent section we analyze and discuss these results.

3.1. *Membership*

3.1.1. *Spectral Types*

For most of our targets, spectral types were derived by comparison with spectral standards and/or other cluster members whose spectral types were known, in a similar manner to that of Kirkpatrick et al. (1999) and Martín et al. (1999), using several spectral indices defined on the red side of the optical spectrum. These standards, whose spectral types go from K7 to M8, were observed with the same spectral setup. In the case of the echelle spectra collected with the MIKE spectrograph, we estimated the spectral types using the TiO band-head, which starts at 7053 Å. The depth of this feature is very sensitive to the effective temperature, and it is an excellent spectral type indicator. In this case, in addition to our IC 2391 candidates, we observed standards of almost every spectral subclass in the vicinity of M5, with half-subclass steps. A visual inspection, comparing IC 2391 members with the standard stars and verifying the spectral classification by direct comparison among the IC 2391 objects themselves, was also carried out. We believe that the uncertainty of the IC 2391 spectral types we have derived is on the order of half a subclass.

Five of our fainter targets ($I_C \sim 20$ mag), observed with HYDRA II, have spectra with a very low S/N, and we have not attempted spectral classification.

The spectral type of several of our brighter candidates is in strong disagreement with membership in the cluster, since they do not correspond to the value expected from the optical and infrared colors. This is the case of two stars—CTIO-002 and CTIO-067—of K spectral type, probable background giants. These two stars, as well as the fainter objects, have no detectable Hα in emission or the line is seen in absorption (see § 3.1.2).

3.1.2. Hα *Emission*

The strength of the Hα emission can be used as a criterion to establish the membership of a cluster candidate. As stated before, two objects of K spectral type, warmer than the expected values from their colors, lack Hα emission, and therefore they can be classified as likely nonmembers. The same argument is valid for three of the five faint objects located at the end of the cluster sequence ($I_C \sim 20$), since we would have expected, at least, some emission. Note, however, that this criterion is a statistical one, and membership cannot be completely ruled out for these three objects or confirmed for the other two. In any case, the data suggest that there is a strong pollution rate for this range, about 60%.

The comparison of the Hα distribution between clusters of different ages is displayed in Figure 5. For clarity, we have only included the cluster associated to the multiple star σ Ori (Wolk 1996) and the α Per cluster. The data come from Béjar et al. (1999), Barrado y Navascués et al. (2001d, 2002b, 2003), Zapatero Osorio et al. (2002), Prosser (1992, 1994), Prosser & Randich (1998), and Stauffer et al. (1999). We note that the σ Ori cluster, with an age close to 5 Myr, has a significant number of stellar and substellar members with Hα far beyond the limits of the figure and might contain about 20% of classical T Tauri stars and substellar analogs (Barrado y Navascués et al. 2003; Barrado y Navascués & Martín 2003; Jayawardhana et al. 2003), which are characterized, among other things, by strong, asymmetric, and broad Hα emission lines. We find that the distribution of Hα emission in IC 2391 is very similar to that for the somewhat older α Per cluster.

Only one star belonging to IC 2391 stands out in the figure, CTIO-059. This object is shown with the average value corresponding to the two observations we carried out in 1999 January at CTIO, but in fact it was observed on two consecutive nights and showed very different values (49.5 and 18.8 Å; see Paper I). Therefore, it seems that we detected a flare in that cluster member at that time.

Figure 6 displays the Hα equivalent width versus time. There might be some variability on short timescales, within the same night. This variability could be related with rotation (see, e.g., possible modulation due to rotation in CTIO-038 or CTIO-074). Variability on a longer timescale might be present too, but the data set is too sparse and we cannot confirm this at the present time. In any case, it would be very interesting to compare this information with light curves derived for the same objects.

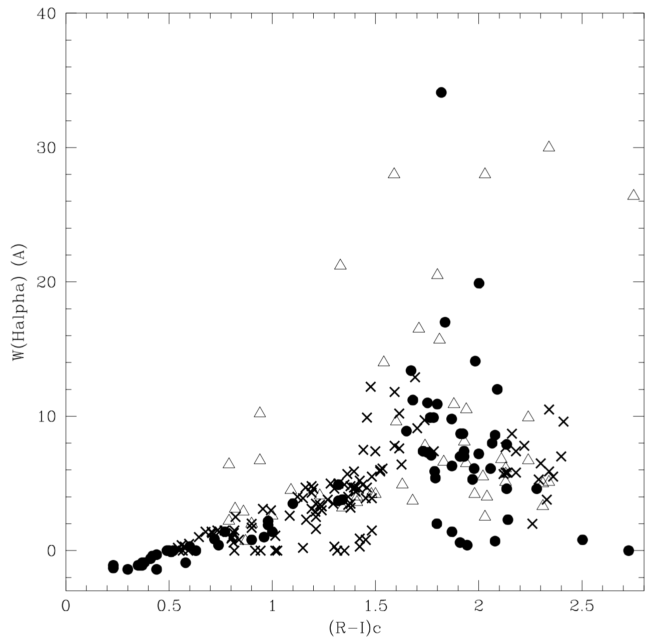

Fig. 5.—Comparison between the Hα equivalent widths vs. the $(R-I)_C$ color index for several clusters. Triangles, circles, and crosses represent data from σ Orionis, IC 2391, and α Per clusters, respectively. Note that a significant fraction of σ Ori members (eight in this color interval) have Hα larger than 40 Å. This is likely an affect of accretion by a disk (Barrado y Navascués et al. 2003; Barrado y Navascués & Martín 2003).

3.1.3. *Sodium Doublet at* 8200 Å

We have also measured the equivalent widths of the sodium doublet at 8200 Å. The strength of this alkali feature is sensitive to gravity (see, e.g., Martín et al. 1996). Since IC 2391 members are much younger than field objects of similar spectral types and should have larger radii, it is possible to use this characteristic as a youth indicator. All our targets but one (CTIO-046) have W(Na I) in agreement with a young age and therefore with membership. The large equivalent width measured in CTIO-046 indicates that it is a more evolved object, which confirms our other indications that this star is probably not a member of the cluster.

3.1.4. *Lithium at* 6707 Å

Figures 7 and 8 display the area around Li I λ6708 for all our spectra. The vertical dashed line indicate the location of this feature. In some cases, the S/N is indeed good, and lithium is unambiguously detected; see, e.g., the cases of CTIO-145 and 038 (1999 January), CTIO-081 (1999 March), CTIO-195, 192, and 026 (2002 December), and CTIO-160 (2003 March). Other cases, such as the two spectra of CTIO-077 (1999 January and March), are less certain. In any case, the new data allow us a significant improvement in the determination of the location of the LDB (§ 3.2).

3.1.5. *Confirmed Members at the Substellar Limit*

So far, including the data published in Paper I, we have collected medium-resolution spectroscopy for 47 candidate members (out of the 206 identified in Paper II and a handful of brighter objects). The membership of another three (CTIO-040, CTIO-094, and VXR 27) was rejected in Paper I. Our targets

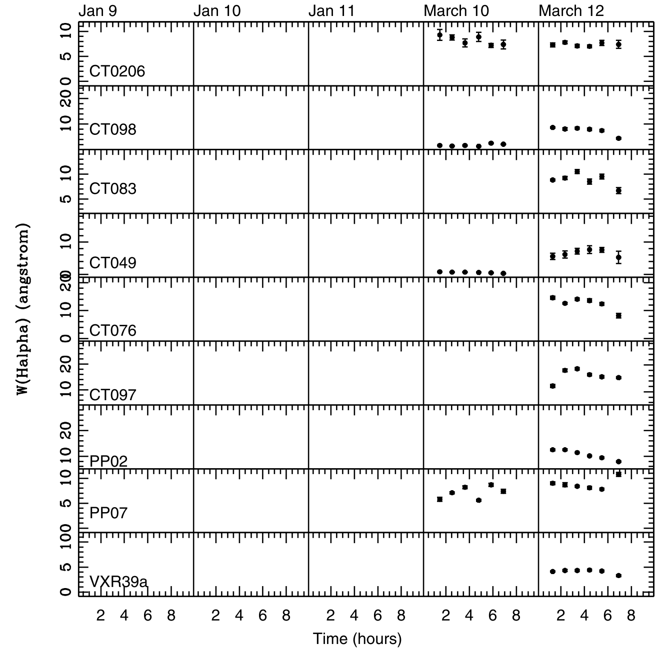

FIG. 6*a*

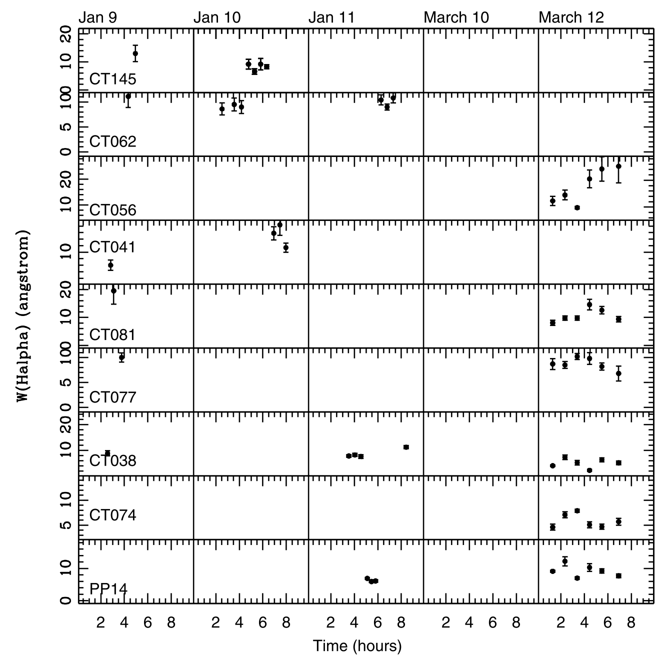

FIG. 6*b*

FIG. 6.—Hα equivalent width vs. time. The data correspond to the (*a*) 1999 January and (*b*) March campaigns. Note the date on top of each panel.

were selected from those that were classified as probable and possible members in Paper II on the basis of their optical and infrared photometry (132 objects in total). In that study, we estimated the pollution rate for that subsample—candidates identified for the first time in Paper II—as 25%. Of the 47 spectroscopically observed candidates (including some VXRP and PP objects), nine were classified as nonmembers (the membership of three out of this nine, namely, CTIO-040, CTIO-094, and VXR 27, was rejected in Paper I) and another five as possible members (four from the CTIO sample). Of those, 38 objects (the CTIO-XXX) were discovered and presented in Paper II, while another six brighter objects came from previous studies (from Patten & Simon 1996 and Patten & Pavlovsky 1999). Therefore, taking into account these 38 CTIO objects, including four possible members in the CTIO sample, and CTIO-040 and CTIO-094, the nonmembers discussed in Paper I, the pollution rate is in the range 20%–30% for the CTIO sample, depending on how the possible members are counted.

3.2. *Lithium Depletion Boundary and Cluster Age*

3.2.1. *Lithium Equivalent Width versus Magnitudes and Colors*

The initial LDB for IC 2391 was located at $I_{\rm C} = 16.2 \pm 0.2$ and $(R - I)_{\rm C} = 1.91$ in Paper I. Figures 7 and 8 contain the area around the Li I λ6708 doublet for the bona fide members. The initial estimate of the LDB location is confirmed, but there are two stars—PP 07 and CTIO-206—that show lithium in their spectra despite the fact they are brighter than the LDB. Figures 9*a* and 9*b* display CMDs using optical and infrared data. We have used $I_{\rm C}$ from Paper II in the *y*-axis for the first case and K_s from 2MASS in the second. In both cases these two stars are clearly above the LDB. Actually, CTIO-206, the fainter of these two, might be a binary composed of two very low mass stars of almost the same mass, which would solve the puzzle. However, the other star, PP 07, is well above the LDB, by about 2 mag. In both cases, the Na I (λ8200) equivalent width is in agreement with a young object.

A similar situation has been discovered in the Pleiades cluster by Oppenheimer et al. (1997), and their interpretation was that the two supposed Pleiades members (HHJ339=HCG 332 and HHJ409=HCG 509) are, in fact, young interlopers in the line of sight. Recently, Deacon & Hambly (2004) have derived membership probabilities for them. Although they are very low ($P = 0.155$ and 0.284, respectively), these values are not conclusive, and membership cannot be completely excluded.

The alternative would be that there is a mechanism that can prevent lithium depletion during the pre–main-sequence phase in M dwarfs. Note that some warmer α Per and Pleiades members (K spectral type) may inhibit lithium depletion using a mechanism related to rotation or magnetic field strength (see, e.g., Soderblom et al. 1993; García López et al. 1994; Randich et al. 1998; D'Antona et al. 1998). However, our medium-resolution spectrum of PP 07 does not seem to be broader than the rest (although it would have been very difficult to detect anything with a projected rotational velocity of less than $\sim$100 km s^{-1}), and its activity in Hα is average compared with other cluster members of the same color or spectral type.

Another, more speculative, possibility is that these two objects are, in fact, bona fide very low mass members of the cluster that have recently swallowed a companion (a brown dwarf). The sudden additional mass accretion could explain their location in these color-magnitudes diagrams and the strong lithium feature in the spectrum. This mechanism has been invoked to explain the tendency among planet-harboring stars to be metal-rich (Santos et al. 2001, 2003; Gonzalez et al. 2001). Possible evidence of planetary engulfment has been presented by Israelian et al. (2001), although it has been called into question by others (Reddy et al. 2002).

In any event, Figure 9 clearly shows the lithium chasm (i.e., the lack of lithium for late K and early M in the cluster). Figure 10 helps to determine with greater degree of accuracy the location of the chasm and, therefore, its cool border, the

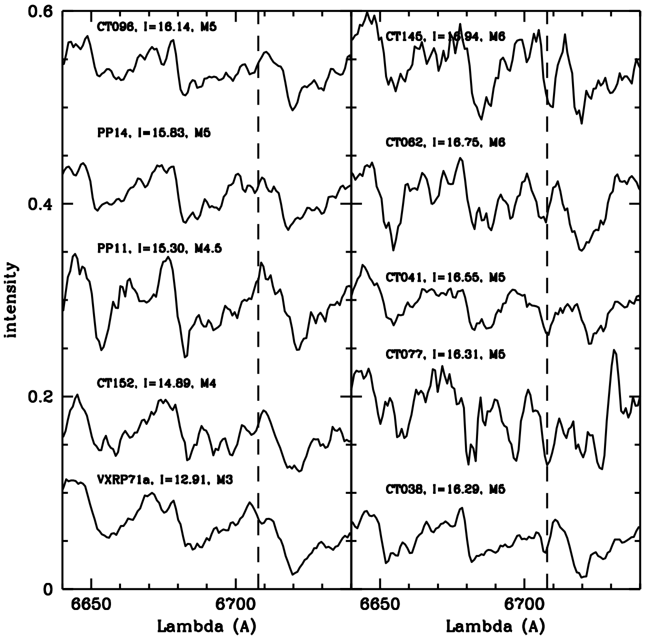

FIG. 7*a*

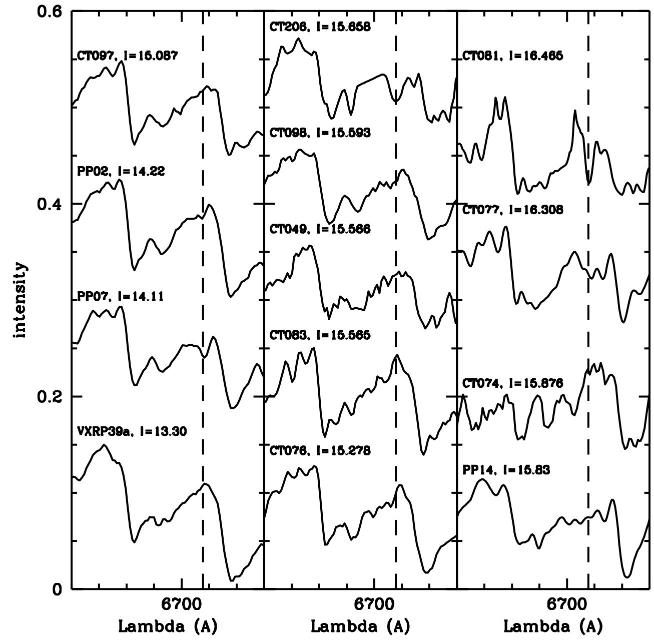

FIG. 7*b*

FIG. 7.—Detail around the Li λ6708 feature for the (*a*) 1999 January and (*b*) March data sets.

LDB. Objects with lithium are displayed with filled symbols (circles for our data, squares for data from Randich et al. 2001), whereas open symbols represent objects without it (triangles for our upper limits). The LDB keeps its location at $(R-I)_{\rm C}^{\rm LDB} \sim 1.9$. Our first detection of lithium is located at $I_{\rm C}=16.286$, whereas the last star without it has a magnitude of $I_{\rm C}=16.144$ ($K_s=13.394$ and 13.587, respectively, if 2MASS data are used instead). Since the adopted distance and reddening are $(m-M)_0 = 5.95 \pm 0.10$ and $E(B-V) = 0.06$, equivalent to $A_I = 0.112$ and $A_K = 0.021$ (Rieke & Lebofsky 1985), these values yield $M(I_{\rm C})^{\rm LDB} = 10.15$ and $M(K_s)^{\rm LDB} = 7.52$.

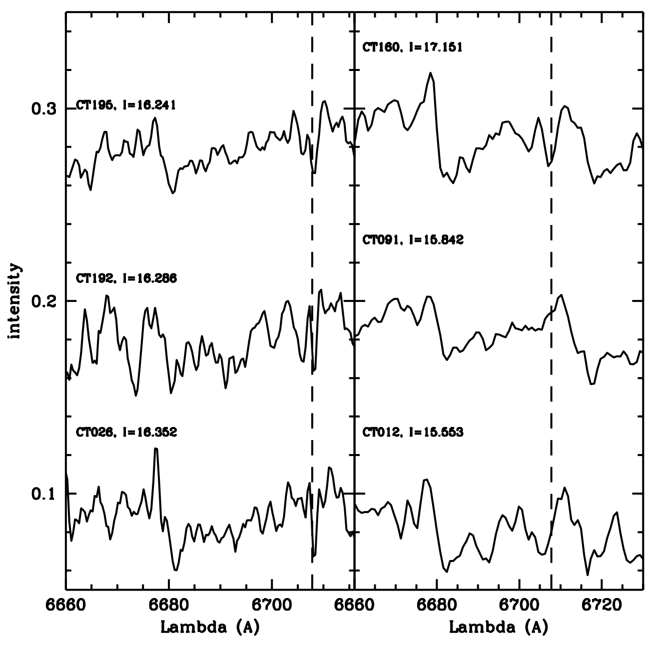

FIG. 8.—Detail of the spectra around the Li λ6708 feature for the (*a*) 2002 December and (*b*) 2003 March spectra (with resolutions of 0.55 and 2.3 Å).

The distance yielded by *Hipparcos* would locate the LDB 0.13 mag fainter than these values.

3.2.2. *Lithium Depletion and a New Lithium Depletion Boundary Age Estimate*

The evolution of the LDB and the lithium chasm with age, from the empirical point of view, is illustrated in Figure 11, where we show a comparison with the three clusters where this type of data is available (IC 2391, α Per and the Pleiades). Additional information can be found in Rebolo et al. (1996); Stauffer et al. (1998, 1999); Martín et al. (1998); Basri & Martín (1999). Note that a detection of the LDB has been attempted in a fourth cluster, NGC 2547, by Oliveira et al. (2003; see also Jeffries et al. 2003), but they were not able to detect it unambiguously.

We have already determined the absolute magnitudes in the $I_{\rm C}$ and K_s filters, where the LDB appears in IC 2391. Using bolometric corrections of $\mathrm{BC}_I = 0.070$ (Bessell 1991; Comerón et al. 2000) and $\mathrm{BC}_K = 2.756$ (Tinney et al. 1993; Leggett et al. 1996), the LDB is located at $M(\mathrm{bol},\ K_s)^{\rm LDB} = 10.229$ and $M(\mathrm{bol},\ I_{\rm C})^{\rm LDB} = 10.251$, or $M(\mathrm{bol})^{\rm LDB} = 10.24$ mag.

We have analyzed in the same way all the data available in the literature for α Per and the Pleiades clusters:

1. In the case of α Per, taking into account a distance modulus of $(m-M)_0 = 6.23$ and $E(B-V) = 0.096$, and assuming that the LDB is defined by AP310, AP322, and AP300 (AP325 might be a binary based on its location in the CMD), we derive $M(I_{\rm C})^{\rm LDB} = 11.42$ and $M(K_s)^{\rm LDB} = 8.31$. In the same way as for IC 2391, $M(\mathrm{bol})^{\rm LDB} = 11.31$ mag.
2. For the Pleiades cluster, the LDB is defined by CFHT-Pl-09, CFHT-Pl-10, Roque 16, and Teide 2 (CFHT-Pl-13). Assuming $(m-M)_0 = 5.60$ and $E(B-V) = 0.04$ (Pinsonneault et al. 1998), we derive $M(I_{\rm C})^{\rm LDB} = 12.18$, $M(K_s)^{\rm LDB} = 8.94$, and $M(\mathrm{bol})^{\rm LDB} = 12.14$ mag.

In all cases, an error of 0.15 mag has been estimated for the location of the LDB, taking into account distances, reddening, and the gap between Li detection and nondetection.

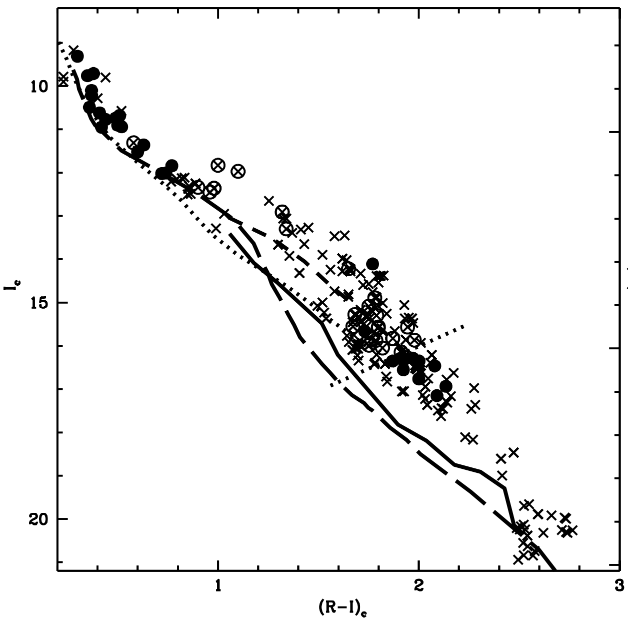

FIG. 9*a*

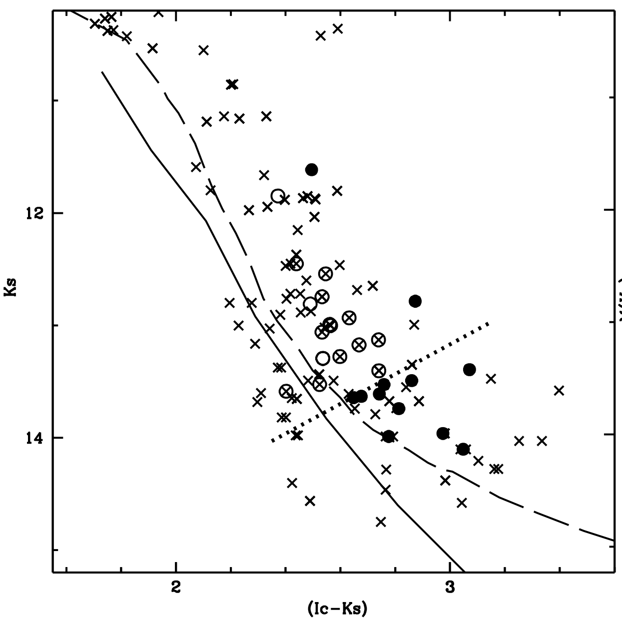

FIG. 9*b*

FIG. 9.—CMDs and the LDB for IC 2391 candidate members. Crosses represent all candidate members from Simon & Patten (1998), Patten & Pavlovsky (1999), and Barrado y Navascués et al. (2001c). IC 2391 members with lithium detection are shows as filled circles, whereas those lacking the Li λ6708 feature are displayed as open symbols. (*a*) We plot different 50 Myr isochrones—short-dashed line for D'Antona & Mazzitelli (1997), long-dashed line for Baraffe et al. (1998), and dotted line for Siess et al. 2000). The solid line represents an empirical ZAMS. (*b*) A 50 Myr isochrone is also included (Baraffe et al. 1998, *long-dashed line*), as well as an empirical ZAMS (*solid line*) and the location of the LDB (*dotted line*).

With these values and the predictions of theoretical models, it is possible to estimate the age of each cluster. Figure 12 displays the absolute magnitudes of an object whose lithium has been depleted almost completely (1% of the original lithium abundance) versus the time. The models correspond to $M(I_C)$ and $M(K_s)$ (I. Baraffe 2003, private communication) and M(bol) (D'Antona & Mazzitelli 1997). Similar diagrams can be created using models by Burrows et al. (1997). The

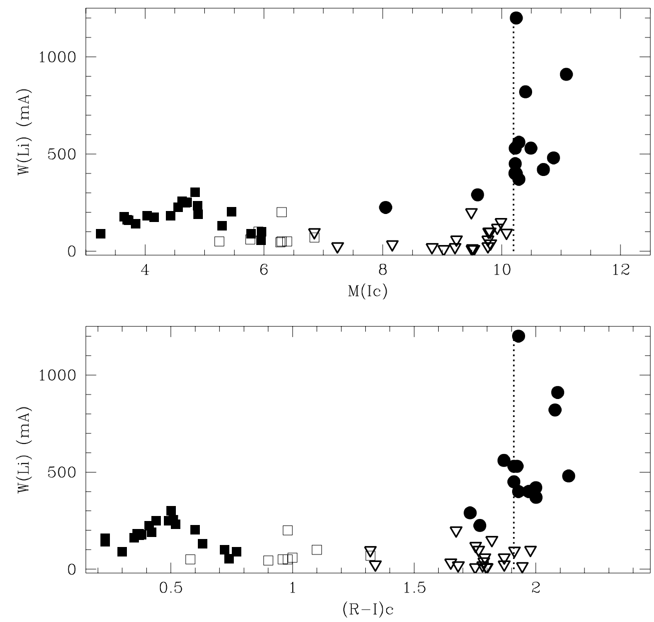

FIG. 10.—Lithium equivalent width vs. the absolute I_C magnitude (*top*) and $(R-I)_C$ color index (*bottom*). Circles and triangles represent data from this work and Barrado y Navascués et al. (1999), whereas squares correspond to data from the literature. Actual data and upper limits are displayed as filled and open symbols, respectively. The vertical dotted line locates the LDB for the cluster.

ages derived are 52, 51, and 46 Myr for IC 2391, 79, 89, and 79 Myr for α Per, and 122, 124, and 153 Myr for the Pleiades. That is, we estimate the plausible ages for these three clusters as 50 ± 5, 85 ± 10, and 130 ± 20 Myr, respectively. Note, however, that Jeffries & Naylor (2001) have reevaluated the error budget for them, both experimental and systematic, and

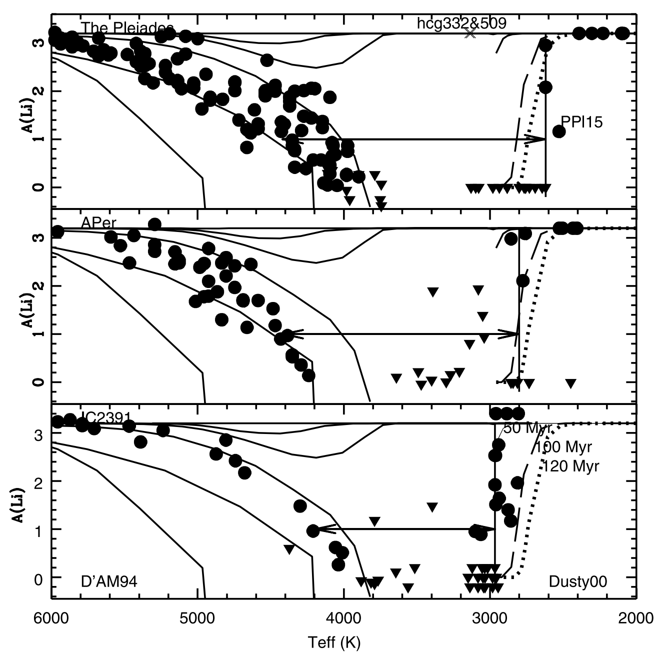

FIG. 11.—Lithium abundance vs. effective temperature. Actual abundances and upper limits are shown as circles and triangles, respectively. Several lithium depletion isochrones from D'Antona & Mazzitelli (1994)—1, 3, 5, 10, 20 and 100 Myr (*left*)—and Chabrier et al. (2000)—50, 100 and 120 Myr (*right*)—are included.

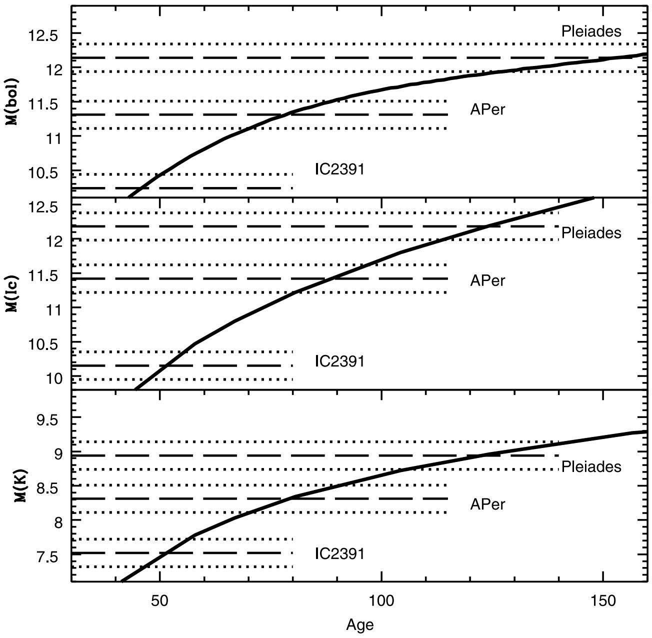

FIG. 12.—Location of the LDB for IC 2391, α Per, and the Pleiades. For the top panel we have used data from D'Antona & Mazzitelli (1997), whereas the other two display results from I. Baraffe (2003, private communication).

estimated that the errors can be significantly larger. As an example, a different I-band bolometric correction [Monet et al. 1992, using a relationship between $(V - I)$ and $(R - I)$ colors] for the LBD in the Pleiades yields an age of 140 Myr instead 153 Myr. If we had used Baraffe's models instead of those from D'Antona & Mazzitelli (1997), the ages derived from the M(bol) would have been 135 or 125 Myr for these two different bolometric corrections. Moreover, the use of *Hipparcos* distance would have added about 3 Myr to the age derived for IC 2391.

Burke et al. (2004) have also revaluated the ages for these three clusters plus NGC 2547 and examined the errors in the analysis. Their values are 55 ± 6, 101 ± 12, and 148 ± 19 Myr for IC 2391, α Per, and the Pleiades (48, 87, and 126 Myr when introducing an ad hoc offset to the I-band bolometric correction). Within the error bars, all these results agree with each other.

As stated in Stauffer et al. (1998, 1999), Barrado y Navascués et al. (1998), and Paper I (see a summary in Barrado y Navascués et al. 1999), these ages are about 50% older than the values obtained by fitting isochrones to the upper part of the main sequence. Recently, Allen et al. (2003) have derived an age for IC 2391 based on the LF of the cluster. They obtained a value, 35 Myr, lower than the LDB age and identical to the main-sequence turn-off age (Mermilliod 1981). By fitting the data published in Paper II with models of the LF, they argue that LF has a peak at $M(I) = 14$–15 mag, which should be produced by the deuterium burning, and that the age cannot be $\sim$50 Myr. Their result supports a recent claim by Song et al. (2002), who state that the LDB age might overestimate the real age for young clusters. However, the analysis by Allen et al. (2003) was carried out prior to our new spectroscopic data, which indicate that the pollution rate in that range ($I_{\rm C} \sim 20$) is very large ($\sim$60 %). The alleged LF peak is not obvious at all now. In addition, Dobbie et al. (2002) have pointed out that a drop in the LF exists around M7-M8 ($T_{\rm eff} \sim 2500$ K), which might be due to dust formation in the atmospheres of these objects. For IC 2391, this happens at about $I_{\rm C} \sim 19.5$ mag.

For these three clusters, the LDBs are located at the spectral types of M5, M6.5, and M6.5 or, in effective temperatures, 3050, 2800, and 2650 K, for IC 2391, α Per, and the Pleiades, respectively. When expressed in mass, using models from Baraffe et al. (1998), they take place at 0.12, 0.085, and 0.075 $M_\odot$, respectively. All the LDB data are summarized in Table 3.

TABLE 3
SUMMARY OF THE LITHIUM DEPLETION BOUNDARY DATA

Parameter	IC 2391	α Per	The Pleiades
$(m - M)_0$	5.95	6.23	5.60
$E(B - V)$	0.06	0.096	0.04
$M(I_{\rm C})$	10.15	11.42	12.18
$M(Ms)$	7.52	8.31	8.94
M(bol)	10.24	11.31	12.14
Spectral type	M5	M6.5	M6.5
$T_{\rm eff}$ LDB (K)	3050	2800	2650
Turn-off age (Myr)	35	50	80–100
LDB age (Myr)	50 ± 5	85 ± 10	130 ± 20
Mass ($M_\odot$)	0.12	0.085	0.075

3.2.3. *The First Confirmed Brown Dwarf in the Cluster*

So far, although a large number of candidate brown dwarfs were presented in Paper II, none of these candidates were established via spectroscopy. This confirmation implies that (1) it is a member of the cluster based on all available criteria, (2) it has a bolometric magnitude that would place it below the substellar mass limit if it were a member of the cluster, and (3) there is a detection of the lithium λ6708 doublet.

Using our new age estimate and models by Baraffe et al. (2002), the interstellar reddening, and the cluster distance, the substellar limit is located at $I_{\rm C} = 17.06$. Several of the targets in this sample are fainter than this value, and their spectroscopic properties agree with membership. However, their spectra are not good enough to have a lithium detection beyond a doubt, which would confirm the substellar nature. Only in one case, CTIO-160 (whose spectral type is M7), is lithium clearly identified and its nature firmly established, making this object the first brown dwarf unambiguously identified in the IC 2391 cluster. Note, however, that error bars in the object photometry and the uncertainties in the models are large enough to change the classification of this object.

3.3. *Mass Function*

We have derived a mass function for IC 2391 using non-dusty models from Baraffe et al. (1998) and the $I_{\rm C}$ magnitudes. Figure 13 depicts our results. We have assumed different ages, ranging from 25 to 50 Myr (these values are close to the turn-off and the LDB ages, respectively). In any case, when expressed as a power law, the index ($\alpha = 0.96 \pm 0.12$) does not depend on the age in this interval (i.e., the derived value is very similar when using these three ages). The MF is valid between a mass of 0.5 $M_\odot$ and the substellar limit. Below 0.072 $M_\odot$, there is a sudden drop, which might be partially explained by the lack of survey completeness beyond $I_{\rm C} \sim 18.5$ for cluster members (0.050 $M_\odot$ for 50 Myr isochrone from Baraffe et al. 1998). However, we have detected a significant number of candidate members with magnitudes around $I_{\rm C} \sim$ 20. Our medium-resolution spectroscopy indicates that despite

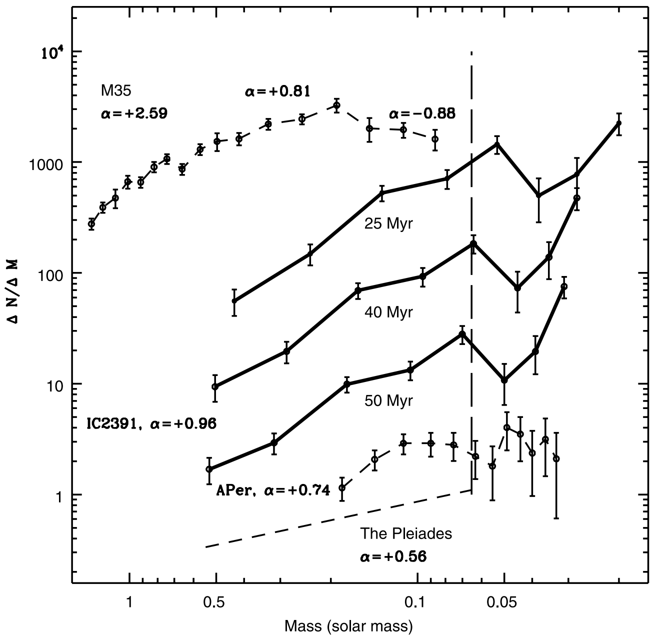

FIG. 13.—Mass functions corresponding to several young open clusters. Those corresponding to IC 2391, computed assuming different ages, are highlighted with a thick, solid line. The vertical segment (*long-dashed line*) represent the completeness limit for our survey.

the strong pollution in this range, about 60%, some seem to be members of the cluster. Therefore, the gap at $I_C \sim 19$, mass $\sim 0.05\ M_\odot$ might be real. Dobbie et al. (2002) and Jameson et al. (2003) have pointed out that several young clusters show a lack of substellar members of M7-M8 spectral type, more or less in the same location as in the case of IC 2391 (see the case of α Per in the same diagram). They explain this fact as an effect of dust formation at this spectral type and its effect in the LF as a new source of opacity, which would decrease the overall luminosity for the cooler objects. In any event, the number of objects discovered so far in the IC 2391 cluster at the low end of the cluster sequence is too low to confirm this possibility.

Figure 13 also contains a comparison with several mass functions corresponding to young clusters of different ages, such as α Per, the Pleiades, and M35, all of them derived in the same manner (see Bouvier et al. 1998; Barrado y Navascués et al. 2001b, 2002a; Barrado y Navascués & Stauffer 2003; Barrado y Navascués 2003). The index of the mass function power law is very similar in all cases, except in the case of the low-mass stellar members of M35, a very rich cluster, where some mass segregation might have taken place as a result of its older age (175 Myr in the turn-off age scale; Barrado y Navascués et al. 2001a).

4. CONCLUSIONS AND SUMMARY

By collecting medium-resolution spectroscopy for a significant fraction of IC 2391 candidate members discovered in Paper II, we have established the membership for most of them via their spectral types and Hα emission properties, including dependence with spectral type and variability in a short timescale. In addition, we have studied the presence of the lithium doublet at 6708 Å, located the LDB in the CMD, and with the help of theoretical models, derived an age estimate, 50 ± 5 Myr. The same study was carried out in other two clusters, namely, α Per and the Pleiades. Our new age estimate is 85 ± 10 and 130 ± 20 Myr. We have also derived an IMF for the low-mass end of the IC 2391 cluster, fitting a power law with an index of $\alpha = 0.96 \pm 0.12$.

We thank the staff of the CTIO 4 m and Magellan telescopes for outstanding support. The anonymous referee has indeed contributed to the improvement of the paper. D. B. y N. is indebted to the Spanish "Programa Ramón y Cajal," AYA2001-1124-CO2 and AYA2003-05355 programs. R. J. acknowledges support from NSF grant AST 02-05130. This publication makes use of data products from the Two Micron All Sky Survey.

REFERENCES

Allen, P. R., Trilling, D. E., Koerner, D. W., & Reid, I. N. 2003, ApJ, 595, 1222
Baraffe, I., Chabrier, G., Allard, F., & Hauschildt, P. H. 1998, A&A, 337, 403
———. 2002, A&A, 382, 563
Barrado y Navascués, D. 2003, in Rev. Mexicana Astron. Astronf. Conf. Ser. 16, Science with the GTC 10 m Telescope, ed. J. M. Rodríguez Espinosa, F. Grazón López, & V. Melo Martín (Mexico: Univ. Nacional Autónoma de Mexico), 261
Barrado y Navascués, D., Béjar, V. J. S., Mundt, R., Martín, R., Rebolo, R., Zapatero Osorio, M. R., & Bailer-Jones, C. A. L. 2003, A&A, 404, 171
Barrado y Navascués, D., Bouvier, J., Stauffer, J. R., Lodieu, N., & McCaughrean, M. J. 2002a, A&A, 395, 813
Barrado y Navascués, D., Deliyannis, C. P., & Stauffer, J. R. 2001a, ApJ, 549, 452
Barrado y Navascués, D., & Martín, E. L. 2003, AJ, 126, 2997
Barrado y Navascués, D., & Stauffer, J. R. 2003, in IAU Symp. 211, Brown Dwarfs, ed. E. Martín (San Francisco: ASP), 155
Barrado y Navascués, D., Stauffer, J. R., & Bouvier, J. 1998, Ap&SS, 263, 239
Barrado y Navascués, D., Stauffer, J. R., Bouvier, J., Jayawardhana, R., & Cuillandre, J. C. 2004, ApJ, 610, 1064
Barrado y Navascués, D., Stauffer, J. R., Bouvier, J., & Martín, E. L. 2001b, ApJ, 546, 1006
Barrado y Navascués, D., Stauffer, J. R., Briceño, C., Patten, B., Hambly, N. C., & Adams, J. D. 2001c, ApJS, 134, 103 (Paper II)
Barrado y Navascués, D., Stauffer, J. R., & Patten, B. M. 1999, ApJ, 522, L53 (Paper I)
Barrado y Navascués, D., Zapatero Osorio, M. R., Béjar, V. J. S., Rebolo, R., Martín, E. L., Mundt, R., & Bailer-Jones, C. A. L. 2001d, A&A, 377, L9
Barrado y Navascués, D., Zapatero Osorio, M. R., Martín, E. L., Béjar, V. J. S., Rebolo, R., & Mundt, R. 2002b, A&A, 393, L85
Basri, G., Marcy, G. W., & Graham, J. R. 1996, ApJ, 458, 600
Basri, G., & Martín, E. L. 1999, ApJ, 510, 266
Basri, G., Mohanty, S., Allard, F., Hauschildt, P. H., Delfosse, X., Martín, E. L., Forveille, T., & Goldman, B. 2000, ApJ, 538, 363
Becker, W., & Fenkart, R. 1971, A&AS, 4, 241
Béjar, V. J. S., Zapatero Osorio, M. R., & Rebolo, R. 1999, ApJ, 521, 671
Bessell, M. S. 1979, PASP, 91, 589
———. 1991, AJ, 101, 662
Bouvier, J., Stauffer, J. R., Martín, E. L., Barrado y Navascués, D., Wallace, B., & Béjar, V. 1998, A&A, 336, 490
Burke, C. J., Pinsonneault, M. H., & Sills, A. 2004, ApJ, 604, 272
Burrows, A., et al. 1997, ApJ, 491, 856
Chabrier, G., Baraffe, I., Allard, F., & Hauschildt, P. 2000, ApJ, 542, L119
Comerón, F., Neuhëuser, R., & Kaas, A. A. 2000, A&A, 359, 269
Cutri, R. M., et al. 2003, 2MASS All-Sky Catalog of Point Sources (Pasadena: IPAC/Caltech)
D'Antona, F., & Mazzitelli, I. 1994, ApJS, 90, 467
———. 1997, Mem. Soc. Astron. Italiana, 68, 807
D'Antona, F., Ventura, P., Mazzitelli, I., & Zeppieri, A. 1998, Mem. Soc. Astron. Italiana, 69, 575
Deacon, N. R., & Hambly, N. C. 2004, A&A, 416, 125
Dobbie, P. D, Pinfield, D. J., Jameson, R. F., & Hodgkin, S. T. 2002, MNRAS, 335, L79
García López, R. J., Rebolo, R., & Martín, E. L. 1994, A&A, 282, 518
Gonzalez, G., Laws, C., Tyagi, S., & Reddy, B. E. 2001, AJ, 121, 432

Israelian, G., Santos, N. C., Mayor, M., & Rebolo, R. 2001, Nature, 411, 163
Jameson, R. F., Dobbie, P. D., Pinfield, D. J., Hodgkin, S. T. 2003, in IAU Symp. 211, ed. E. L. Martín (San Francisco: ASP), 171
Jayawardhana, R., Ardila, D. R., Stelzer, B., & Haisch, K. E., Jr. 2003, AJ, 126, 1515
Jeffries, R. D., & Naylor, T. 2001, in ASP Conf. Ser. 243, From Darkness to Light: Origin and Evolution of Young Stellar Clusters, ed. T. Montmerle & P. André (San Francisco: ASP), 633
Jeffries, R. D., Oliveira, J. M., Barrado y Navascués, D., Stauffer, J. R. 2003, MNRAS, 343, 1271
Kirkpatrick, D., et al., 1999, ApJ, 519, 802
Leggett, S. K. 1992, ApJS, 82, 351
Leggett, S. K., Allard, F., Berriman, G., Dahn, C. C., & Hauschildt, P. H. 1996, ApJS, 104, 117
Martín, E. L. Basri, G., Gallegos, J. E., Rebolo, R., Zapatero-Osorio, M. R., & Bejar, V. J. S. 1998, ApJ, 499, L61
Martín, E. L., Rebolo, R., & Zapatero Osorio, M. R. 1996, ApJ, 469, 706
Martín, E. L., et al. 1999, AJ, 118, 2466
Mermilliod, J.-C. 1981, A&A, 97, 235
Monet, D. G., Dahn, C. C., Vrba, F. J., Harris, H. C., Pier, J. R., Luginbuhl, C. B., & Ables, H. D. 1992, AJ, 103, 638
Oliveira, J. M., Jeffries, R. D., Devey, C. R., Barrado y Navascués, D., Naylor, T., Stauffer, J. R., & Totten, E. J. 2003, MNRAS, 342, 651
Oppenheimer, B. R., Basri, G., Nakajima, T., & Kulkarni, S. R. 1997, AJ, 113, 2134
Patten, B. M., & Pavlovski, C. M. 1999, PASP, 111, 210
Patten, B. M., & Simon, T. 1996, ApJS, 106, 489
Pinsonneault, M. H., Stauffer, J., Soderblom, D. R., King, J. R., & Hanson, R. B. 1998, ApJ, 504, 170
Prosser, C. P. 1992, AJ, 103, 488
Prosser, C. P. 1994, AJ, 107, 1422
Prosser, C. P., & Randich, S. 1998, Astron. Nachr., 319, 215
Randich, S., Martín, E. L., García López, R. J., Pallavicini, R. 1998, A&A, 333, 591
Randich, S., Pallavicini, R., Meola, G., Stauffer, J. R., & Balachandran, S. C. 2001, A&A, 372, 862
Rebolo, R., Martín, E. L., Basri, G., Marcy, G. W., & Zapatero-Osorio, M. R. 1996, ApJ, 469, L53
Reddy, B. E., Lambert, D. L., Laws, C., Gonzalez, G., & Covey, K. 2002, MNRAS, 335, 1005
Rieke, G. H., & Lebofsky, M. J. 1985, ApJ, 288, 618
Robichon, N. M., Arenou, F., Mermilliod J.-C., & Turon, C. 1999, A&A, 345, 471
Santos, N. C., Israelian, G., & Mayor, M. 2001, A&A, 373, 1019
Santos, N. C., Israelian, G., Mayor, M., Rebolo, R., & Udry, S. 2003, A&A, 398, 363
Siess, L., Dufour, E., & Forestini, M. 2000, A&A, 358, 593
Simon, T., & Patten, B. M. 1998, PASP, 110, 283
Skrutskie, M. F., et al. 1997, in The Impact of Large Scale Near-IR Sky Surveys, ed. F. Garzon et al. (Dordrecht: Kluwer), 25
Soderblom, D. R., Jones, B. F., Balachandran, S., Stauffer, J. R., Duncan, D. K., Fedele, S. B., & Hudon, J. D. 1993, AJ, 106, 1059
Song, I., Bessell, M.S., & Zuckerman, B. 2002, ApJ, 581, L43
Stauffer, J. R., Schultz, G., & Kirkpatrick, J. D. 1998, ApJ, 499, L199
Stauffer, J. R., et al. 1999, ApJ, 527, 219
Tinney, C. G., Mould, J. R., & Reid, I. N. 1993, AJ, 105, 1045
Wolk, S. J. 1996, Ph.D. thesis, Univ. New York at Stony Brook
Zapatero Osorio, M. R., Béjar, V. J. S., Pavlenko Ya., Rebolo, R., Allende Prieto, C., Martín, E. L., & García López, R. J. 2002, A&A, 384, 937